APPLICATIONS OF HIGH-THROUGHPUT SCREENING TOOLS FOR THERMOELECTRIC MATERIALS

[1] W. Wong-Ng, [1]H. Joress, [1]J. Martin, [1]Y. Yan, [2]J. Yang, [1]M. Otani, [3]E. L. Thomas, [1]M.L. Green, and [1]J. Hattrick-Simpers

[1]MML, NIST, Gaithersburg, MD 20899
[2]GM Research Center, Warren, MI 48090
[3]Air Force Research Laboratory, WPAFB, OH 45433

ABSTRACT

The increased research and development on thermoelectric materials in recent years has been driven primarily by the need for improved efficiency in the global utilization of energy resources. To facilitate the search for new thermoelectric materials, we have developed a high-throughput thermoelectric screening system for combinatorial thin films. This screening system is comprised of two tools, one for measuring the Seebeck coefficient and resistance via an automated multiprobe apparatus, and another for measuring thermal effusivity by a frequency domain thermoreflectance technique. Using these systems, we are able to make measurements for calculating the thermoelectric power factor ($S^2\sigma$, where S = Seebeck coefficient, σ = electrical conductivity) and thermal conductivity of over 1000 sample-points within 6 hours for each instrument. This paper provides examples of our current studies on both oxide and intermetallic materials.

INTRODUCTION

Due to the high gas price and green house emission effect in recent years, there are desperate needs to have alternate energy capabilities and environmentally friendly technologies. Thermoelectric materials have demonstrated the potential for widespread applications in areas of waste heat recovery and solid-state refrigeration. The efficiency and performance of thermoelectric power generation or cooling is related to the dimensionless figure of merit (ZT) of the thermoelectric materials, given by $ZT = S^2\sigma T/\kappa$, where T is the absolute temperature, S is the Seebeck coefficient, σ is the electrical conductivity ($\sigma = 1/\rho$, ρ is electrical resistivity), and k is the thermal conductivity [1]. ZT is directly related to the performance of a thermoelectric material and is the reference by which these materials are judged. The Seebeck coefficient is an important indicator for power conversion efficiency. Thermoelectric materials with desirable properties (i.e., high ZT >>1), are characterized by high electrical conductivity, high Seebeck coefficient, and low thermal conductivity.

Until about 10 years ago, only a small number of materials have been found to have practical industrial thermoelectric applications because of generally low thermoelectric efficiencies. Increased attention to research and development of thermoelectric materials has been partly due to the dramatic increase of the ZT values of materials being discovered in bulk and thin film form [2, 3]. Additional novel materials include quantum well films [4] and quantum dot films [5] that have been reported to yield ZT as high as 2.5.

The goal of this paper is to summarize our recent efforts on the development of high-throughput thermoelectric metrology, including a tool suite for screening the Seebeck coefficient, resistance, and thermal conductivity of combinatorial films. Demonstration of the

applications of these tools on the combinatorial composition-spread films on cobalt oxide systems and the study of the homogeneity of bulk inter-metallic compounds will be given.

A SUITE OF SCREENING TOOLS FOR COMBINATORIAL FILMS[1]

For large-scale applications of thermoelectric technology, continued efforts to identify novel materials and to optimize the properties of existing materials are crucial. The combinatorial state-of-the-art synthesis approach is an efficient technique to systematically investigate the thermoelectric properties as a function of composition in complex multi-component systems. This method typically involves fabricating film libraries with compositions varying between two or three different end-member materials on a substrate using physical vapor deposition techniques, followed by evaluation of the film libraries with high-throughput screening tools [6-10]. We have developed a high-throughput screening system for thermoelectric material exploration using combinatorial films prepared with a continuous spread of compositions. This system consists of a power factor screening tool and a thermal conductivity screening tool [11].

Power Factor Screening tool

The high-throughput power factor screening tool that we developed can be used to measure electrical resistance and the Seebeck coefficient [12, 13]. Measurements are fully automated by a computer (Fig 1). The salient features of the power factor screening tool consist of a probe to measure Seebeck coefficient and electric conductivity, an automated translation stage to scan the film in the *x*-*y*-*z* directions, and various voltage measuring instruments. The measurement probe consists of four gold-plated spring probes as sample contacts, a heater to generate temperature differences between two of the spring probes, two thermometers to measure the temperature of these probes, two insulators, and two copper plates. To achieve accurate Seebeck coefficient measurements, a spring probe is placed directly on each copper plate, and the other spring probe is attached on the insulator. The four probes can be arranged either in a square array or in a colinear fashion. A thermometer is attached on each copper plate and a heater is attached on one of the copper plates. Electrical conductivity is measured by the conventional 4-probe van der Pauw method [14] (Fig. 2). All Seebeck coefficient measurements were conducted at room temperature and at $\Delta T = 4.1$ K. It takes about 20 seconds to measure both electric conductivity and Seebeck coefficient for each sample point. This probe allows us to measure electric conductivity and Seebeck coefficient of over 1000 sample points within 6 hours.

In order to estimate the accuracy of our screening tool, we compared the Seebeck coefficients of several bulk and film samples using our screening probe and a traditional, one-sample-at-a-time system (PPMS, Quantum Design[a], with the Thermal Transport Option at room temperature). As seen in Fig.3, measurements using these two instruments are in excellent agreement on a number of representative samples, including films and bulk materials. These results suggest that the scanning probe is reliable and sufficiently accurate as a screening tool for Seebeck coefficients of combinatorial samples.

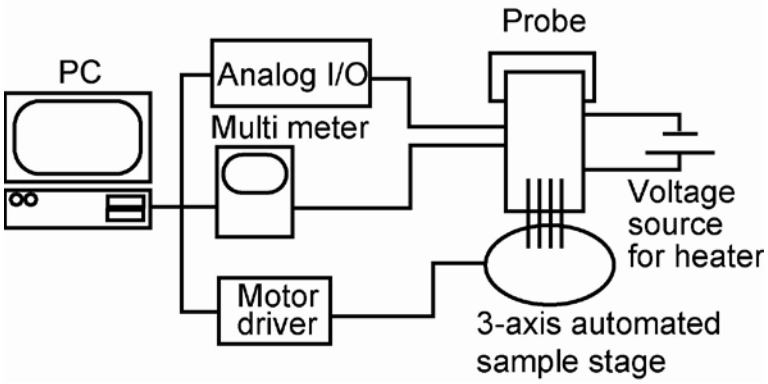

Fig. 1. Schematic diagram of the power factor screening system

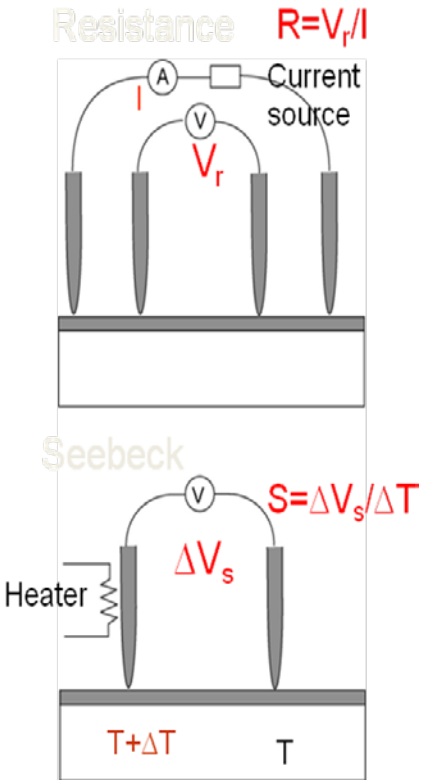

Fig. 2. Schematic of the screening probe to measure electrical conductivity and Seebeck coefficient.

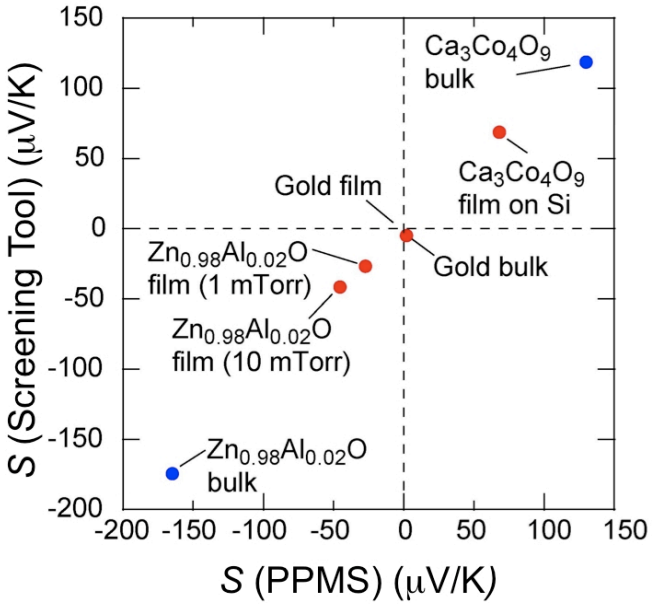

Fig 3. Comparison between Seebeck coefficients measured on several samples, including bulk and film, with our screening tool and a thermal transport option of physical property measurement system (PPMS). The bulk samples are gold foil, polycrystalline $Zn_{0.98}Al_{0.002}O$, and polycrystalline $Ca_3Co_4O_9$. The film sample fabricated by PLD are gold film, $Ca_3Co_4O_9$ film, and two $Zn_{0.98}Al_{0.002}O$ films grown at 1.3 and 13 Pa..

We demonstrated the high-throughput screening of Seebeck coefficient and electrical conductivity using the ternary (Ca, Sr, La)$_3Co_4O_9$ composition-spread films using $Ca_3Co_4O_9$, $Ca_2LaCo_4O_9$, and $Ca_2SrCo_4O_9$ as targets [12, 13]. The composition-spread films were fabricated with a pulsed laser deposition system by the continuous-composition-spread technique. Figure 4 gives the results of the power factor screening of this system (depicted as a conventional ternary diagram). It is clear that the power factor data reach a maximum between the Sr-rich region and the La-rich region. Substitution of the trivalent La^{3+} for the divalent Ca^{2+} is expected to decrease the hole concentration, leading to increasing Seebeck coefficient in the La-rich region. On the other hand, substitution of Sr^{2+} for Ca^{2+} leads to an increase of electrical conductivity and an insignificant change of Seebeck coefficient. This is because the substitution of a larger divalent Sr^{2+} cation for a smaller divalent Ca^{2+} cation would not change the carrier concentration but it would change the carrier mobility by lattice deformation.

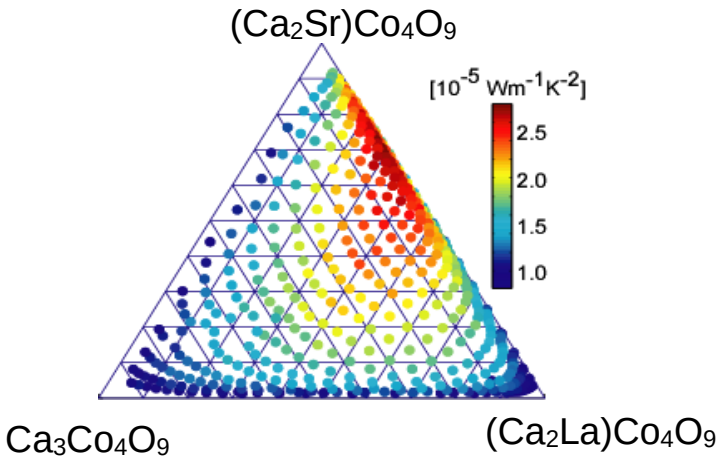

Fig. 4. Power factor of the composition-spread $(Ca_{1-x-y}Sr_xLa_y)_3Co_4O_9$ film ($0 < x < 1/3$ and $0 < y < 1/3$).

We further demonstrated the applications of the screening tool with a quaternary system by extending the ternary system by adding the Mg-cobaltite component. The chemical formula for the 4 targets are $Ca_3Co_4O_9$, $(Ca_2La)Co_4O_9$, $(Ca_2Sr)Co_4O_9$, and $(Ca_2Mg)Co_4O_9$. The quaternary diagram of the composition-spread $(Ca_{1-x-y-z}Sr_xLa_yMg_z)_3Co_4O_9$ film ($0 < x < 1/3$, $0 < y < 1/3$, and $0 < x< 1/3$) was constructed using eleven ternary films. We were able to make these 11 films (about 6000 data points) in about one week. The Seebeck coefficient diagram of this composition-spread film is shown in Fig. 5a. The Seebeck coefficient variation with valence is shown in Fig. 5b. Similar to the previous example, as the valence of the cations increases, the Seebeck coefficient increases because doping with the La^{3+} cation decreases the hole concentration, leading to also a decrease of electrical conductivity.

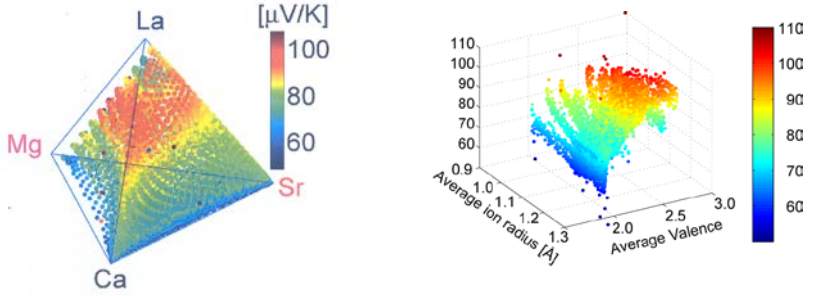

(a) (b)

Fig. 5a. Seebeck coefficient of the composition-spread $(Ca_{1-x-y-z}Sr_xLa_yMg_z)_3Co_4O_9$ film ($0 < x < 1/3$, $0 < y < 1$, and $1/3$, $0 < z < 1$); Ca=$Ca_2CaCo_3O_9$, Sr= $Ca_2SrCo_3O_9$, La=$Ca_2LaaCo_3O_9$, Mg=$Ca_2MgCo_3O_9$. Fig. 5b, Seebeck coefficient variation with valence.

The screening tool has been used to evaluate the homogeneity of three industrially important bulk samples. The first example is screening the homogeneity of a single crystal of S-substituted Bi_2Te_3 (Fig. 6a). The structure is rhombohedral and can be best described as having

quintuple layers of atoms (Te-Bi-Te-Bi-Te) stacked along the *c*-axis [15]. The structure can be considered as having quasi 2D electron layers with van der Waals planes in between each group of the quintuple layers. We have studied the crystal structure at three different locations of this 4.5 cm long crystal, and have screened the Seebeck coefficient along the long axis of the crystal.

The crystal was found to have a concentration gradient along the long-axis. The structure result shows the S and Te concentration are approximately 50:50, but slightly Te-rich (Fig. 6b). In all three compositions that we studied, the Te site in the middle of the quintuple layer in Bi_2Te_3 is occupied by only S, whereas the gap position of Te is occupied by mixed S/Te. The Te has the highest concentration in position #1 ($Bi_2(Te_{1.58(1)}S_{1.42(1)})$, followed by position #2 ($Bi_2(Te_{1.53(1)}S_{1.47(1)})$, and the least in position #3 ($Bi_2(Te_{1.52(2)}S_{1.48(2)})$. In other words, there is slightly more Te in the gap Te/S sites in position #1 than those in positions #2 and #3 .This correlates well with the Seebeck coefficient values (Fig. 7), namely, the higher the Te concentration, the higher the Seebeck coefficient.

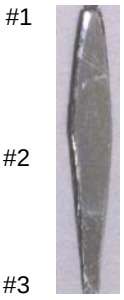

Fig. 6a. Dimension of the $Bi_2(Te,S)_3$ crystal (about 4.5 cm long)

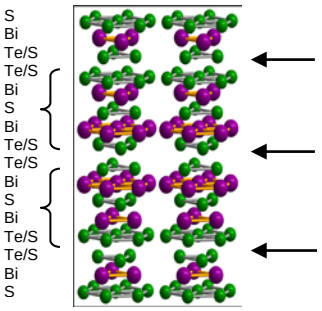

Fig. 6b. Structure of $Bi_2(Te,S)_3$ (← indicates the position of the van der Waals planes)

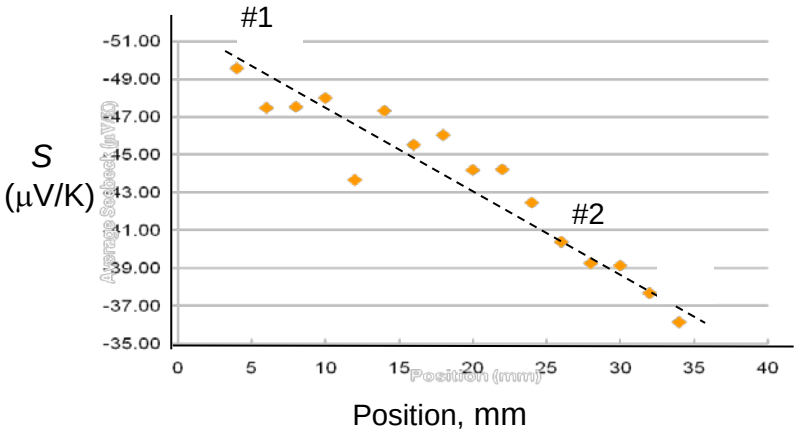

Fig. 7. Seebeck coefficient as a function of distance along the c-axis of the crystal

The second example (in the form of rectangular bars of approximately 2.5 mm x 2.5 mm x 10 mm) is a Type-I clathrate, $Ba_8(Ni,Pt,Pd,Zn)Ga_{13}Ge_{46}$ [16] (Fig. 8), and the third example is a double-filled skutteruide $(Ba,Yb)Sb_4Co_{12}$ [17, 18] (Fig. 9). $Ba_8(Ni,Pt,Pd,Zn)Ga_{13}Ge_{46}$ has an "open" structure that can host guest atoms inside the crystallographic voids. The "rattling" Ba atoms inside the large Ge/Ga cages scatter phonons and thus reduce thermal conductivity. The measurement positions are parallel to the thermal gradient. Each data point was collected after a 30 second stabilization period. A total of 13 scanned data points on $Ba_8(Ni,Pt,Pd,Zn)Ga_{13}Ge_{46}$ gives an average Seebeck coefficient value of -67 μV/K with a 4.5 % (3.0 μV/K) standard deviation. The $(Ba,Yb)Sb_4Co_{12}$ (a skutterudite) sample is also in the form of rectangular bars of approximately 2.5 mm x 2.5 mm x 10 mm. $(Ba,Yb)Sb_4Co_{12}$ has a cubic structure that consists of six 4-membered Sb-rings that are almost parallel to the cell edges. The two large voids in the unit cell can be filled with "rattling" atoms (Ba and Yb ions). Based on the screening of 16 data points, the average Seebeck coefficient for $(Ba, Yb)Sb_4Co_{12}$ is –128 μV/K with a 2 % (2.4 μV/K) standard deviation. Therefore we conclude that both $Ba_8(Ni,Pt,Pd,Zn)Ga_{13}Ge_{46}$ and $(Ba, Yb)Sb_4Co_{12}$ are essentially homogenous samples, as no systematic change in the Seebeck coefficient was observed as a function of position.

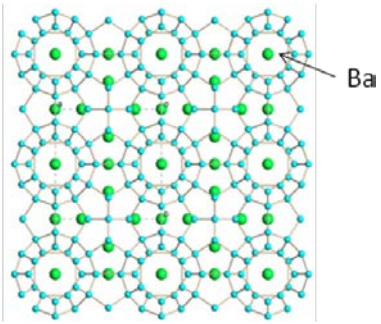

Fig. 8. Planar view of the Type-I clathrate crystal structure showing the two different polyhedra (20-atom cage and 24-atom cage) that form the unit cell.

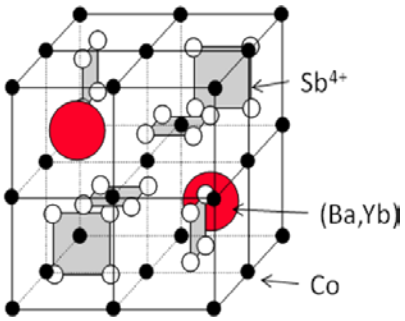

Fig. 9. Structure of the skutterudite $(Ba, Yb)Sb_4Co_{12}$ showing the Sb_4 rings and the voids in the unit cell where the mixed (Ba, Yb) ions reside.

Thermal conductivity screening tool (Frequency-domain thermoreflectance technique)

A scanning thermal effusivity measurement system using the frequency domain thermoreflectance technique has been developed [11]. The thermoreflectance technique is based on the relationship between the change in the optical reflection coefficient of a material and the change in its temperature through periodic heating. By using a metal for the film layer, this method can measure thermal effusivity of ceramics, metals, glass, and plastics. The thermal effusivity measurement system can rapidly and locally (10 micrometer spot size) measure the thermal effusivity of combinatorial (composition-spread) films.

Figure 10 gives a schematic of the scanning thermal effusivity frequency system that includes two laser diodes, a compensating network, a voltage source heater, and an *x*-*y*-*z* axis automated sample stage driven by a motor driver. The sample, which is a thermoelectric film or a bulk sample with a smooth surface, is first coated with a thin molybdenum layer (usually about 100 nm thick), then is locally heated by an intensity-modulated heating laser; the thermal response of the film is detected by the reflected beam of a second (probe) laser. The reflected probe signal is detected by a balance detector. The amplitude and phase difference between signal and reference signal from the pulse generator are obtained by a lock-in amplifier.

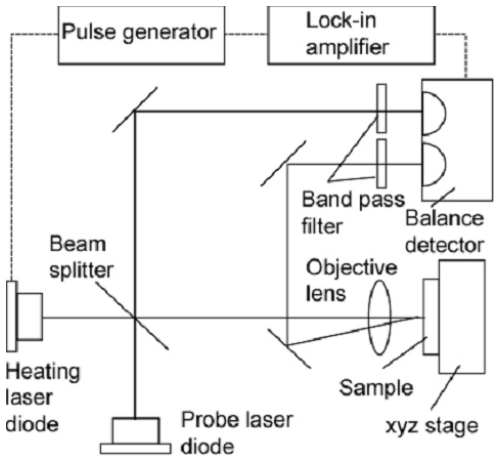

Fig. 10. Schematic diagram of the thermal effusivity screening system (frequency domain thermoreflectance technique)

The thermal effusivity b can be derived from the phase lag, δ, between the thermoreflectance and the heating laser signals. Thermal effusivity is related to thermal conductivity as

$$b = (\kappa c \rho)^{1/2}, \qquad (1)$$

where c is the specific heat, ρ is the density, and κ is thermal conductivity. By choosing the modulation frequency of 1 MHz, we obtained a calibration curve of the phase lag of five bulk samples of which the thermal effusivity values are known: SiO_2, $SrTiO_3$, $LaAlO_3$, Al_2O_3, and Si. The linear dependence of the phase lag on thermal effusivity of these five compounds can be expressed in the following equation,

$$b = -402.34\ \delta + 26352, \qquad (2)$$

where b is the thermal effusivity. If the δ value for an unknown material can be measured experimentally, one can estimate b using equation (2).

We successfully estimated the thermal conductivity value for a 800nm/(100nm Mo) thick conventional $Ba_2YCu_3O_{6+x}$ film on a $SrTiO_3$ substrate. Using equation (1), the thermal effusivity was estimated to be 1370 $Js^{1/2}M^{-2}K^{-1}$ (δ = 62.1 º). The thermal conductivity of the $Ba_2YCu_3O_{6+x}$ film was then determined (c= 430 $J.kg^{-1}K^{-1}$[19], and ρ= 6.38 $g.cm^{-3}$ [20]) to be 12.0 $Jm^{-1}K^{-1}s^{-1}$, which agrees reasonably well (within 10 %) with the reported value of 12.9 $Jm^{-1}K^{-1}s^{-1}$ [19].

To assess the application of the tool for 2-dimensional screening, we determined the δ values of a Si sample in the *yz*-direction (with a 100 nm-thick Mo metallic film on the surface). Using equation (2) with the c, ρ values of 0.713 $Jg^{-1}K^{-1}$ [21] and 2.3290 $g\text{-}cm^{-3}$ [21], respectively, and the measured δ values, we obtained the thermal effusivity and thermal conductivity values of the Si sample in an area of approximately 1 mm x 1 mm in increments of 100 μm. The resulting average κ is (165 ± 15) $Wm^{-1}K^{-1}$, which is within 8 % of the literature reported value of 156 $Wm^{-1}K^{-1}$ [21]. Using this tool, we plan to study the thermal properties of combinatorial film systems in the near future.

FUTURE DEVELOPMENTS

Our continuing development of the power factor screening tool for the thermoelectric combinatorial films focuses on the improvement of its performance. There are three limitations to the current screening tool configuration [12, 13]. First, it is difficult to measure materials with low electrical conductivity (i.e., $<10^{-1}$ $(\Omega cm)^{-1}$ for a 200 nm thin film) and low value of Seebeck coefficient (<5 μV/K) due only to limitations of the homemade current source and voltage meter. Although these limitations do not hamper our ability to screen thermoelectric materials, we could extend our measurement capability by upgrading those two components. Second, the spatial resolution of our screening tool is about 2 mm, corresponding to the distance between two spring probes. If the electrical conductivity of the sample drastically changed over a very short length scale, measurements at a sample point might be affected by its neighbors. We plan to improve this resolution. Third, measurements can be carried out only at room temperature at present. We are currently developing an improved instrument that is capable of high temperature (up to 600 °C) measurement.

[1]Certain commercial equipment, instruments, or materials are identified in this paper in order to specify the experimental procedure adequately. Such identification is not intended to imply recommendation or endorsement by the National Institute of Standards and Technology, nor is it intended to imply that the materials or equipment identified are necessarily the best available for the purpose.

REFERENCES

[1] T.M. Tritt, Thermoelectrics Run Hot and Cold, Science, **272**, 1276-1277 (1996).
[2] K.F. Hsu, S. Loo, F. Guo, W. Chen, J.S. Dyck, C. Uher, T. Hogan, E.K. Polychroniadis, and M.G. Kanatzidis, Cubic $AgPb_mSbTe_{2+m}$: Bulk Thermoelectric Materials with High Figure of Merit, Science, **303**, 818-821 (2004).
[3] R. Venkatasubramanian, E. Siivola, T. Colpitts, and B. O'Quinn, Growth of one-dimensional Si/SiGe heterostructures by thermal CVD, Nature, **413**, 597-602 (2001).
[4] S. Ghamaty, and N.B. Eisner, **"**Development of Quantum Well Thermoelectric films, Proceedings of the 18th International Conference on Thermoelectrics, Baltimore, MD, pp. 485-488 (1999).
[5] M.S. Dresselhaus, G. Chen, M.Y. Tang, R.G. Yang, H. Lee, D.Z. Wang, Z.F. Ren, J.P. Fleurial, and P. Gogna, Enhanced Thermopower in PbSe Nanocrystal Quantum Dot Superlattices, Adv. Mater., **19**, 1043-1053 (2007).
[6] R. Funahashi, S. Urata, and M. Kitawaki, Exploration of n-type oxides by high throughput screening, Appl. Surf. Sci., **223**, 44-48 (2004).
[7] T. He, J.Z. Chen,T.G. Calvarese, M.A. Subramanian, Thermoelectric properties of $La_{1-x}A_xCoO_3$ (A = Pb, Na), Solid State Sciences, **8**, 467-469 (2006).
[8] R. B. Van Dover, L. F. Schneemeyer, R. M. Fleming, Discovery of a useful thin-film dielectric using a composition-spread approach, Nature, **392**, 162 (1998).
[9] T. Fukumura, M. Ohtani, M. Kawasaki, Y. Okimoto, T. Kageyama, T. Koida, T. Hasegawa, Y. Tokura, H. Koinuma, Rapid construction of phase diagram for doped Mott insulators with a composition-spread approach, Appl. Phys. Lett., **77**, 3426-3428 (2000).
[10]H. M. Christen, S. D. Silliman, and K. S. Harchavardhan, Continuous compositional-spread technique based on pulsed-laser deposition and applied to the growth of epitaxial films, Rev. Sci. Instrum., **72**, 2673-2678 (2001).
[11]M. Otani, E. Thomas, W. Wong-Ng, P. K. Schenck, K.-S. Chang, N. D. Lowhorn, M. L. Green, and H. Ohguchi, A High-throughput Screening System for Thermoelectric Material Exploration Based on a Combinatorial Film Approach, Jap. J. Appl. Phys, **48**, 05EB02 (2009).
[12]M. Otani, N.D. Lowhorn, P.K. Schenck, W. Wong-Ng, and M. Green, A high-throughput thermoelectric Screening Tool for Rapid Construction of Thermoelectric Phase Diagrams, Appl. Phys. Lett., **91**, 132102-132104 (2007).
[13] M. Otani, K. Itaka, W. Wong-Ng, P.K. Schenck, and H. Koinuma, Development of high-throughput thermoelectric tool for combinatorial thin film libraries, Appl. Surface Science, **254**, 765-767 (2007).
[14]L.J. van der Pauw, Philips Tech. Rev., A Method of Measuring the Resistivity and Hall Coefficient on Lamellae of Arbitrary Shape, **20**, 220-224, (1958).
[15] P.M. Lee and L. Pincherle, "The Electronic Band Structure of Bismuth Telluride," Pro. Phys. Soc., **81**, 461 (1963); P.W. Lange, Naturwissenschaften **27** 133 (1939).
[16] C. Uher, Skutterudites: Prospective Novel Thermoelectrics in Semiconductors and Semimetals, Semiconductors & Semimetals, **69**, 139-253 (2001).
[17] X. Shi, H. Kong, C.-P. Li, C. Uher, J. Yang, J.R. Salvador, H. Wang, L. Chen, and W. Zhang, Low thermal conductivity and high thermoelectric figure of merit in n-type $Ba_xYb_yCo_4Sb_{12}$ double-filled skutteruide, Appl. Phys. Lett. **92**, 182101 (2008).

[18] X. Shi, J.R. Salvador, J. Yang, and H. Wang, Thermoelectric Properties of *n*-Type Multiple-Filled Skutterudites, J. Electronic Mater. **38**(7), 930-933 (2009).
[19] T. Yagi, N. Taketoshi, and H. Kato, Distribution analysis of thermal effusivity for sub-micrometer YBCO thin films using thermal microscope, Physica C, **412-414**, 1337-1342 (2004).
[20] W. Wong-Ng, R.S. Roth, L.J. Swartzendruber, L.H. Bennett, C.K. Chiang, F. Beech, and C.R. Hubbard, X-ray powder characterization of $Ba_2YCu_3O_{7-x}$, Adv. Ceram. Mater., Vol. **2**(3B), Ceramic Superconductors, ed. W. J. Smothers, Am. Ceram. Soc., Westerville, OH, p. 565 (1987).
[21] Robert Hull, Editor, Properties of Crystalline Silicon, INSPEC, The Institution of Electrical Engineers, London, p. 165 (1999).